Thermal conductivities of three-dimensionally woven fabric composites

J. Schuster, D. Heider, K. Sharp, M. Glowania

Accepted Manuscript

Thermal conductivities of three-dimensionally woven fabric composites

J. Schuster, D. Heider, K. Sharp, M. Glowania

PII: S0266-3538(08)00103-6
DOI: 10.1016/j.compscitech.2008.03.024
Reference: CSTE 4005

To appear in: *Composites Science and Technology*

Received Date: 17 December 2007
Revised Date: 12 March 2008
Accepted Date: 17 March 2008

Please cite this article as: Schuster, J., Heider, D., Sharp, K., Glowania, M., Thermal conductivities of three-dimensionally woven fabric composites, *Composites Science and Technology* (2008), doi: 10.1016/j.compscitech.2008.03.024

Thermal conductivities of three-dimensionally woven fabric composites

J. Schuster[a,e], D. Heider[b], K. Sharp[c] and M. Glowania[d]

[a]University of Applied Sciences Kaiserslautern, Carl-Schurz Str. 10-16, 66953 Pirmasens, Germany, Email: jens.schuster@fh-kl.de, Tel.: +49 (6331) 2483-49, Fax: -50

[b]University of Delaware, Center for Composite Materials, Newark DE 19716, USA

[c]3TEX, 109 MacKenan Drive, Cary NC 27511, USA

[d]RWTH Aachen, Institut für Textiltechnik, Eilfschornsteinstr. 18, 52062 Aachen, Germany

[e]Corresponding author

Keywords: Textile Composites, Thermal properties, Modeling, Finite element analysis

Abstract

This study investigates the effect of three-dimensional fiber reinforcement on the out-of-plane thermal conductivity of composite materials. Composite preforms 3-D orthogonally woven with pitch carbon yarns and plied copper wires in thickness direction. After infusion, using a Vacuum-Assisted Resin Transfer Molding process, the measured out-of-plane thermal conductivities of the resultant composites showed significant increase compared to a typical laminated uniaxially or biaxially reinforced composite. Although the through thickness thermal conductivity of the samples increased with through thickness fiber volume fraction, the values did not match those predicted by a simple rule of mixture. Using Finite Element models to better understand the behavior of the composite material,

improvements to an existing analytical model were performed to predict the effective thermal conductivity as a function of the composite material properties and in-contact thermal material properties.

1. Introduction

Fiber based composites offer the unique ability to tailor material properties locally. Localized matrix or fiber architecture changes can meet local mechanical, electrical, or thermal loads within a component or vehicle, without weight penalty or resort to additional external structures. Such integral materials reduce the number of components leading to not only more elegant designs, but also to structures that are less costly to manufacture. Local strength, stiffness, conductivity, or other properties can be tailored using expensive fibers or matrices, without large cost penalties, since only small amounts of expensive materials must be used. For these and other reasons, composites have replaced metals in a wide range of aircraft structures, realizing considerable weight savings as well as associated cost and performance improvements. However, certain parts of even the most composite intensive aircraft have remained metallic where advantages of the metal parts could not be met or surpassed by available composite systems. These include locations where toughness and the thermal conductivity of the metals justify the weight penalties.

Traditional laminated uniaxial or biaxial composites have low through thickness thermal conductivities, which limit their use in a variety of aerospace applications. Leading edges in supersonic aircraft wings, inlet or exhaust areas of gas turbine engines, light weight heat exchangers, electronics packaging materials, hydraulic pump enclosures, and electro-

magnetic interference (EMI) enclosures all are subject to localized thermal loads which must be transferred through part thickness to adjacent cooler areas for subsequent radiation/convection, in part to mitigate internal stresses induced by reducing the thermal gradient across the part thickness. One common approach to increasing the through thickness conductivity of a composite, namely loading the resin with thermally conductive particles, can increase the conductivity only insignificantly. Also the use of expensive carbon nanotubes can increase the very low matrix thermal conductivity only by a factor of 10 [1]. One alternative approach of achieving significant increase in the through-thickness thermal conductivity is to manufacture composites based on 3-D woven fiber architectures where the through-thickness fibers have high thermal conductivities. One commercially available fabric of this kind is 3WEAVE™ from 3TEX.

2. Description of 3WEAVE™

The multi-rapier, 3-D orthogonal weaving process, 3WEAVE® was originally developed at the NC State University College of Textiles [2] and further refined and enhanced at 3TEX [3]. As illustrated in Figure 1, this process places several layers of fill (y-directional) and warp (x-directional) yarns in x-y plane without any crimp (contrary to conventional 2-D weaving process), thus providing straight bi-directional in-plane reinforcement. Then, the multiple layers of warp and fill yarns are interlaced by a set of "*Z*"-yarns, which holds the fabric together. The "*Z*"-yarns provide a desirable level of out-of-plane strength, so the layers of warp and fill yarns cannot separate. The amount of "*Z*"-fibers can be varied from less than 1% to more than 30% of the total fiber amount in the preform. Using the 3WEAVE®-process, fabrics have been produced with thickness up to 2 inches (5 cm), and

widths up to 72 inches (183 cm). The 3WEAVE®-process does not subject the warp- and fill-directional fibers to significant bending loads, thus improving the ability to use of rather brittle fibers, such as highly thermally conductive pitch yarns over traditional 2-D. Further, it is possible to fabricate integral complex shapes into 3-D woven preforms. Importantly, different fiber kinds can be hybridized in a 3-D woven integral preform. Selective placement of fiber types through the preform can make a composite material with gradually changing properties. This could be used for tailoring density, stiffness, strength, thermal expansion, thermal conductivity, and other properties.

3. Predictive models for thermal conductivity of composites

The development of models for the description of heat transfer processes dates to the 19th century. Maxwell found that thermal conduction problems can be regarded similarly to problems of electrical conductivity, permittivity, and magnetic permeability [4]. His findings were based on the previous work of Fourier who presented his Théorie de la Chaleur in 1807/1808. Maxwell and Lord Rayleigh published a book on heat transfer (of fluids, bodies, inifinite solids) in 1891 [5]. In the following year, Rayleigh introduced a model to describe electrical conductivities of media [6]. Hugo Fricke stretched the electric conductivity modeling to disperse systems in 1924 which can be treated similarly to thermal conductivity and Bruggeman extended this approach to thermal conductivity in 1935 [7, 8]. Sugawara and Yoshozawa and Brailsford and Major published their research on thermal conductivity of aggregates and porous materials [9, 10]. One early transfer of these results to unidirectional reinforced plastics for longitudinal and transverse thermal conduction was accomplished by Thornburg and Pears in 1965 [11]. However, the simple

approaches in modeling for the transverse thermal conductivity achieved only a moderate level of precision, in part due the neglect of interface conditions. In 1967 Springer and Tsai published another model for the prediction of the thermal conductivity normal to circular fibers based on shear properties [12]. Clayton proposed a model that can only iteratively be solved [13]. In 1983, Hashin extended the shear property approach to define upper and lower bounds for through thickness thermal conductivity of transversely isotropic materials [14]. In 1986, Beneviste and Miloh published a model which accounts different shapes of particles (short orthotropic fibers) and bounding conditions [15], while Hatta and Taya studied the thermal conductivity of coated-fiber composites [16]. One year later, Chawla developed a model for transversly isotropic composites having a thermal mismatch in the interface region and Hasselman and Johnson improved the Hatta/Taya-model by incorporating a thermal barrier resistance for the interface [17, 18]. In 1993, this model was extended to orthotropic carbon fibers by Hasselman [19]. In that same year, Farmer-Covert published an improvement of Rayleighs model [20]. Clayton's model was improved by Krach and Advani in 1996 to consider voids [21].

In addition to models for laminated uniaxial composites, models for conventionally woven fabric based composites have been developed. The first model for glass-fiber woven fabric composites was published by Knappe and Martinez-Freire in 1965 [22]. This model is applicable only for a fiber volume fraction up to 50% and provides useful predictions for fiber volume fractions up to 40 %. In 1992, Dasgupta and Agarwal published an extensive paper on thermal conductivities of plain-weave balanced fabric composites, where

"balanced" means to identical properties in warp and weft direction of the fabric [23]. Ning and Chou have refined the Dasgupta/Agarwal-model for unbalanced fabrics in 1995 [24].

More recently, a model for commingled yarn performs was published by Thomann et.al. in 2004. Unfortunately, this model necessitates the knowledge of a number of material parameters such as number of fibers, and average distance of fibers, and initial void content [25]. Also, Turias et.al. proposed the utilization of artificial neural networks to estimate thermal conductivities of unidirectional composites [26].

All of these models apply only for two-dimensional in-plane reinforcements and they yield a maximum thermal out-of-plane thermal conductivity of a composite material approximately four times higher than the matrix conductivity for neat resins ($K_{Cmax} \approx 0.8$ W/(m K)) . In order to model transverse (out-of-plane) thermal conductivities of three-dimensional fiber assemblies, these models have to be combined in a parallel connection, as also suggested by Kulkarni and Brady for carbon/carbon composites [27]. More specifically, the model for longitudinal thermal conductivity of Thornburg and Pears for "*Z*"-fibers and the commonly used transverse conductivity model of Hatta and Taya for orthotropic x-and y-fibers are applied [11, 16].

$$k_{11} = (1-\nu_F)k_M + \nu_F k_{Fa} \tag{1}$$

$$k_{22} = k_M + \frac{k_M (k_{Fr} - k_M)\nu_F}{k_M + (1-\nu_F)(k_{Fr} - k_M)\frac{1}{2}} \tag{2}$$

$$k_{33Comp} = k_{11}\,\delta_{z-fiber} + k_{22}\,(1-\delta_{z-fiber}) \tag{3}$$

with $\delta_{z-fiber} = \frac{\nu_{Fz}}{\nu_F}$ (4)

and k_{11} - thermal conductivity of UD-Laminate in 1,1-direction (longitudinal)

k_{22} - thermal conductivity of cross-ply laminate in 2,2-direction (transverse)

k_{33Comp} - thermal conductivity of composite in 3,3-direction

k_M - thermal conductivity of matrix

k_{Fa} - axial thermal conductivity of fiber

k_{Fr} - radial thermal conductivity of fiber

ν_F - fiber volume fraction

ν_{Fz} - fiber volume fraction of z-fibers

4. Thermal Conductivity Measurements

Thermal conductivity measurements were performed with a measuring cell built in-house at the Center for Composite Materials at the University of Delaware according to ASTM E 1225 – 04 allowing measurements of circular samples with a diameter of 2" (50.8 mm) at thicknesses from 2 until 50 mm [28, 29]. A heat flux, approximately 2000 W/m^2, was introduced by a cartridge heater. Three thermistors in the top meter bar are used to measure heat flux which is assumed to be constant while traveling through the sample into the lower meter bar where a fourth thermistor recorded temperature. The top meter bar is insulated with foam and additionally shielded by a guard heater to prevent radial heat loss. Conductivity paste (OT-201 from Omega with K = 2.3 W/(m K)) was used in order to facilitate coupling and to reduce interfacial thermal resistance between meter bars and samples. The bottom meter bar contacted a cool plate to provide a heat sink with a constant

temperature T_{sink} beneath the bottom plate. All of the thermistor information was evaluated by a LabView-based program. Calibration measurements were performed on isotropic specimens to determine the accuracy of the measuring cell. Using stainless steel references, the thermal resistance R_{int} at the interfaces from meter bars and sample was determined to be 533 (K mm^2)/W. Once the calibration measurements were completed, eleven composite samples made of 3WEAVE®-preforms infused by resin in a VARTM-process were tested [31 -34], the results of which are shown in Table 1 and 2. A typical sample (here from Fabric A) with a thickness of 10 mm is shown in Fig. 2. Both sides of samples were ground parallel prior to testing. The theoretical thermal conductivities K of these samples were calculated according to eqn. 1 – 4 and are shown in Table 2. The measured data compared with literature values of isotropic samples and theoretical derived conductivities of the composite samples are depicted in Fig. 3.

It can be seen that results for isotropic materials match their reference values well. However, the measured values for the composite samples with z-fiber reinforcement differ drastically from theoretically derived thermal conductivities despite the standard deviation for all material tests was less than ± 5 %. This leads to the conclusion that a simple model consisting of a parallel connection between out-of-plane conductivities of in-plane fibers and "*Z*"-fibers can not be applied for these materials.

5. FE-Analysis

To get a better understanding of this result, the heat flow through a composite unit cell (thickness 10 mm) encompassing a single copper fiber sandwiched between two meter bars

was modeled by finite elements (COSMOSWorks™) with a strictly vertical heat flux of q" = 500 W/m^2 and T_{sink} = 20 °C. Using this volume FE model with triangled meshes, variations in the ν_{fz} of the copper fibers in the composite can be coupled with variations in the thermal conductivity of the meter bar. The copper volume fraction of the composite was varied between 0 and 100% and the thermal conductivity of the meter bar was also varied in steps between 0.1 and 1000 W/(m K). Thus, the effect of volume fraction and thermal conductivity on the measurement of thermal conductivity could be determined (Fig. 4). It is obvious that the measured thermal conductivity is influenced not only by the volume fraction but also by the connecting meter bar material. Thus a simple rule of mixtures estimate of the composite transverse thermal conductivity appears to be the upper bound for a sample where the thermal conductivities of the connecting materials approach infinity.

Section views taken of heat flux simulations through the meter bar-composite system taken from Fig. 5 show a strong influence of that the meter bar thermal conductivity has on the heat flux distribution in the system. All of the above diagrams have the same heat flux passing through the composite. Higher thermal conductivity in the meter bar material increases the proportion of the heat flux through the copper fiber. In contrast, the low conductivity meter bar material allows little heterogenization of the heat flow, so a higher proportion of the heat flux passes primarily through the area of the composite between "*Z*"-fibers. As the thermal conductivity of the meter bar increases, significant heat flow passes through a larger meter bar area near the copper, as seen in the increasing size of the "mushroom" cap near the copper. Therefore, since the thermal conductivities of the

materials in contact with the anisotropic or orthotropic composite sample material has such a large effect on the hear flux, the modeled thermal conductivity derived from temperature data is a system rather than a material property. Further evidence of this effect is proven experimentally in chapter 7.

Fig. 6 also implies that the degree of redirection of heat flux is affected by the "*Z*"-fiber distribution which provide discrete highly conductive heat flux entry points into the composite material. Further FE-simulations of composite samples having the same Cu volume content but distributed in one, four, and eight paths show (Fig. 6), that this distribution influences the resultant thermal conductivity of the sample (Table 3). A FE-analysis of a real sample was not possible due to the computer memory limitations.

6. Improvements to Analytic Model

As described above, two effects unique to heterogeneous materials could be identified:

- Thermal conductivity of the material where the heterogenization of heat flux occurs
- Distribution density of z-fibers

As common in describing properties of composites these effects can be included by introducing factors to the simple rule of mixture, which can be calculated based on geometrical and material properties.

$$K_{3weave} = K_{z-fiber}\,\delta_{z-fiber}\,\eta_{KMat}\eta_{Dens} + (1-\delta_{z-fiber})\,K_{in-planex,y} \quad (5)$$

In this equation, η_{KMat} reflects the influence of the thermal conductivity of the adjoining material and η_{Dens} takes the effect of the fiber distribution density into account.

$$\eta_{Dens} = \frac{d_{Fiber}}{D_{Fiber}} = \frac{d_{Fiber}}{d_{Fiber}\sqrt{\frac{\pi}{4\nu_{z-fiber}}}} = 2\sqrt{\frac{\nu_{z-fiber}}{\pi}} \quad (6)$$

The areal density value can be expressed by ratio of the fiber diameter d_{fiber} and the distances between fibers (D_{fiber}) measured from the center of a fiber. η_{Dens} varies between "0" and "1", and is normalized for the minimum possible fiber distance, obtained by calculating the fiber diameter at the maximum fiber volume fraction for a square array at 78.5 % [35]. To improve the accuracy of this empirical factor, a correcting exponent "a" was introduced By fitting the FE-results to eqn. 5, the value for "a" was determined to 0.5. For a fiber volume fraction $\nu_{z\text{-}fiber}$ of e.g. 5.5 % the density factor becomes 0.514.

$$\eta_{Dens} = \left[2\sqrt{\frac{\nu_{z-fiber}}{\pi}}\right]^{a} = \left[2\sqrt{\frac{\nu_{z-fiber}}{\pi}}\right]^{0.5} \quad (7)$$

Eqn. 7 approximates empirically the effect of increase in diameter of the mushroom cap shaped heat flux area with the thermal conductivity of the meter bar material as be seen in Fig. 5. The dependency of η_{KMat} on the meter bar material can also be derived from the FE-results. A plot of the results of simulations where the thermal conductivity of the meter bar is varied produced a curve that can be described by a vertical shifted hyperbolic tangent function. Both the simulation and the best fit hyperbolic tangent curve are depicted in Fig. 7:

$$\eta_{KMat} = \frac{1}{2}\left[\tanh(\log(0.1K_{Mat})) + 1\right] \quad (8)$$

η_{KMat} becomes e.g. 0.6 for stainless steel as a meter bar material. An empirically approach is required since the analytic solution for two-dimensional heat flux exist only for special cases. As depicted in Fig. 8, at high "*Z*"-fibers volume fractions this approach may not be accurate due to the overlapping of the mushroom cap shape heat flux area not being properly considered. Also, eqn. 6 is valid only until $\nu_{z\text{-fiber}} = 78.5$ %. Nevertheless, usual "*Z*"-fiber contents are lower than 15 %. The results of the improved model are shown in Fig. 9 in comparison to the simple model results proving the accuracy of the model introduced.

7. Experimental validation for η_{KMat}

In order to prove this factor experimentally, isotropic metal references were inserted between sample Fabric A and the lower meter bar. After new determination of the Rint values for the system were completed, required due to the increase in the number of interfaces the results of test measurements for several connecting materials with quite different thermal conductivities (stainless steel, K = 16.2 W/(m K) and copper, K = 390 W/(m K) are depicted in Fig. 10. The test results confirm the assertions in Chap 5 on the influence of the adjoining material on the measured thermal conductivity. Furthermore, these results prove that the ratio of η_{KMat} between of copper and stainless steel is in the range of 1.3 to 1.6 which corresponds well with model results.

8. Discussion, Conclusions, and Perspectives

The thermal conductivity measurements on three-dimensionally reinforced composite samples did not follow the expected rule of mixtures relationship. One explanation of these

results involves the interaction of discrete thermally high conductive heat flux paths in the composite samples with the homogeneous heat flow introduced in the test system under investigation. Thus, the thermal conductivity of a 3-D composite material must be considered as a system property and not a material property due to the influence of the thermal conductivity of the connecting material, the meter bar in the test set-up. Furthermore, the distances between these paths define the ability of the composite system to heterogenize the heat flux and can be expressed by the distance between fibers derived via fiber diameter. Although the development of a purely analytical thermal conduction model for a complex system is unlikely due to the two-dimensional nature of heat flux, the introduction of two factors to the simple rule of mixtures estimations led to reasonalbly accurate model predictions for the samples tested. Experimental data showed that with a "*Z*"-fiber volume content of about 6 % the maximum possible out-of-plane thermal conductivity can be increased by a factor of eight over that of a traditional uniaxial or biaxial laminate composite. This opens the possibility to design composite parts in terms of heat transfer having the thermal conductivity as design aspect to varied by fiber architecture and thus to seen equal to mechanical design criteria such as Young's modulus or strength.

Future investigations shall be aimed on 3WEAVE®-reinforcement with a higher volume fraction of z-fibers and the use of z-fibers with a higher axial thermal conductivity.

Acknowledgements

The work described was conducted as part of United States Air Force SBIR contract FA8650-06-C3616..

References

1 **Bagchi A., Nomura S.** On the Effective Thermal Conductivity of Carbon Nanotube Reinforced Polymer Composites. Composites Science and Technology 2006; 66 (11-12): 1703 - 1712

2 **Mohamed M.H., Zhang Z.** Method of Forming Variable Cross-sectional Shaped Three-Dimensional Fabrics. USP 5,085,252, 1992.

3 **Mohamed M.H., Bogdanovich A.E., Dickinson L.C., Singletary J.N., Lienhart R.R.** A New Generation of 3D Woven Fabric Preforms and Composites. SAMPE Journal 2001; 37 (3): 8-17.

4 **Maxwell J.C.** Electricity and Magnetism. Clarendon Press, 1873

5 **Maxwell J.C., Rayleigh M.A.L.** Theory of Heat. Longmans, Green, and Co. New York, Bombay, and Calcutta, 1891

6 **Rayleigh M.A.L.** On the Influence of Obstacles Arranged in Rectangular Order upon the Properties of a Media. Philosophical Magazine 1892; 34: 481

7 **Fricke H.** A Mathematical Treatment of the Electric Conductivity and Capacity of Disperse Systems. Physical Review 1924; 24: 575 - 587

8 **Bruggemann D.A.G.** Berechnung verschiedener physikalischer Konstanten von heterogenen Substanzen. Analen der Physik 1935; 416 (3): 636 - 664

9 **Sugawara A., Yoshizawa Y.** An Experimental Investigation on the Thermal Conductivity of Consolidated Porous Materials. Journal of Applied Physics 1962; 33 (10): 3135 - 3138

10 **Brailsford A.D., Major K.G.** The Thermal Conductivity of Aggregates of several Phases including porous Materials. British Journal of Applied Physics 1964; (15): 313 - 139

11 **Thornburg J. D., Pears C.D.** Prediction of the Thermal Conductivity of Filed and Reinforced Plastics. ASME Paper 65-WA/HT-4. 1965

12 **Springer G.S., Tsai S.W.** Thermal Conductivities of Unidirectional Materials. Journal of Composite Materials 1967; (1): 166 - 173

13 **Clayton W.A.** Constituent and Composite Thermal Conductivities of Phenolic-Carbon and Phenolic-Graphite Ablators. Proceedings 12th Structures, Structural Dynamics and Material Conference of AIAA/ASME, 1971. p. 1 – 17

14 **Hashin Z.** Analysis of Composite Materials – a Survey. Journal of Applied Mechanics 1983; 50 (9): 481 – 505

15 **Beneviste Y., Miloh T.** The Effective Conductivity of Composites with Imperfect Thermal Contact at Constituent Interfaces. International Journal of Engineering Science 1986; 24 (9): 1537 - 1552

16 **Hatta H., Taya M.** Thermal Conductivity of Coated Filler Composites. Journal of Applied Physics 1986; 59 (6): 1851 - 1860

17 **Chawla K.K.** Composite Materials. Science and Engineering Springer-Verlag New York, 1987

18 **Hasselman D.P.H., Johnson L.F.** Effective Thermal Conductivity of Composites with Interfacial Thermal Barrier Resistance. Journal of Composite Materials 1987; 21 (6): 508-515.

19 **Hasselman D.P.H., Donaldson K.Y., Thomas J.R.** Effective Thermal Conductivity of Uniaxial Composites with Cylindrically Orthotropic Carbon Fibers and Interfacial Thermal Barrier. Journal of Composite Materials **1993;** 27 (6): 637 – 644

20 **Farmer J.D., Covert E.E.** Transverse Thermal Conductance of Thermosetting Materials during their Cure. AIAA 34th SDM Conference, paper 93.1574.CP, 1993, p. 2337 - 2346

21 **Krach A., Advani S.G.** Influence of Void Shape, Void Volume and Matrix Anisotropy on Effective Thermal Conductivity of a Three-Phase Composite. Journal of Composite Materials 1996; 30 (8): 933 - 945

22 **Knappe W., Martinez-Freire P.** Messung und Berechnung der Wärme-leitfähigkeit von Glasfaser/Kunststoff Kunststoffe. 1965; 55 (10): 776 - 779

23 **Dasgupta A., Agarwal R.K.** Orthotropic Thermal Conductivity of Plain-Weave Fabric Composites Using a Homogenization Technique. Journal of Composite Materials 1992; 26 (18): 2736 - 2758

24 **Ning Q.-G., Chou T.-W.** A Closed-Form Solution of the Transverse Effective Thermal Conductivity of Woven Fabric Composites. Journal of Composite Materials 1995; 29 (17): 2280 - 2294

25 **Thomann U.I., Sauter M., Ermanni P.** A Combined Impregnation and Heat Transfer Model for Stamp Forming of Unconsolidated Commingled Yarn Preforms. Composite Science and Technology 2004; 64 (10 – 11): 1637 - 1651

26 **Turias I.J., Gutierrez J.M., Galindo P.L.** "Modelling the Effective Conductivity of an Unidirectional Composite by the use Artificial Neural Networks. Composites Science and Technology 2005; 65 (3 – 4): 609 - 619

27 **Kulkarni M.R., Brady R.P.** A Model of Global Thermal Conductivity in Laminated Carbon/Carbon Composites. Composites Science and Technology 1997; 57 (3): 277 - 285

28 **N.N.** Standard Test Method for Thermal Conductivity of Solids by Means of the Guarded-Comparative-Longitudinal Heat Flow Technique ASTM E 1225-04, 2004

29 **Laubitz M.J.** Axial Heat Flow Methods of Measuring Thermal Conductivity. Compendium of Thermophysical Property Measurement Methods Volume 1, Plenum Press New York and London, 1984

30 **Wetherhold R.C., Wang J.** Difficulties in the Theories for Predicting Transverse Thermal Conductivity of Continuous Fiber Composites. Journal of Composite Materials 1994; 28 (15): 1491 – 1498

31 **Mathur R., Heider D., Hoffmann C., Gillespie Jr. J.W., Advani S.G., Fink B.K.** Flow Front Measurements and Model Validation in the Vacuum-Assisted Resin Transfer Molding Process. Polymer Composites 2001; 22 (4): 477-490

32 **Heider D., Gillespie Jr. J.W.** Automated VARTM processing of large-scale composite structures. Journal of Advanced Materials 2004; 36 (4): 11-17.

33 **Acheson J.A., Simacek P., Advani S.G.** The Implications of Fiber Compaction and Saturation on Fully Coupled VARTM Simulation. Composite Part A 2004; 35:159-169.

34 **Bender D., Schuster J., Heider D.** Flow Rate Control during Vacuum-Assisted Resin Transfer Molding (VARTM) Processing. Composites Science and Technology 2006; 66 (13): 2265 - 2271

35 **Hull D., Clyne TW.** An Introduction to Composite Materials Cambridge University Press, Second Edition, 1996

Figures and Tables

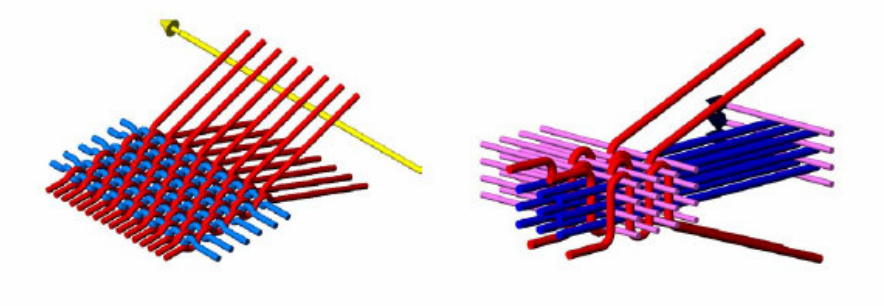

2-D weave formation 3-D (3WEAVE^{TM}) weave formation

Figure 1: *Schematic of the 2-D and 3-D weaving processes*

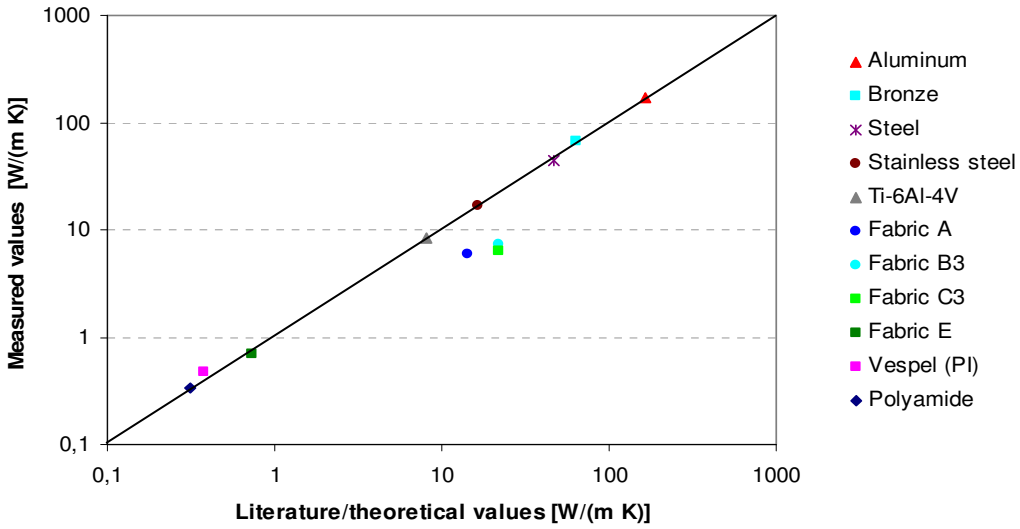

Figure 3: ***Results of thermal conductivity measurements***

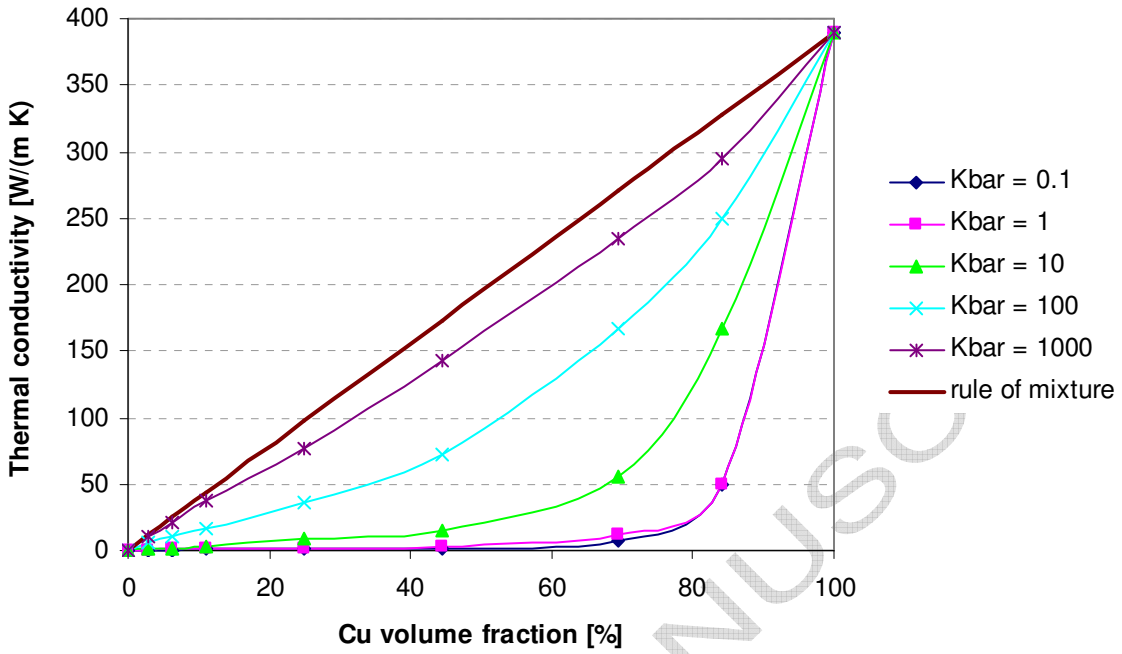

Figure 4: ***Thermal conductivity based on Cu-fiber volume fraction and meter bar material's thermal conductivity***

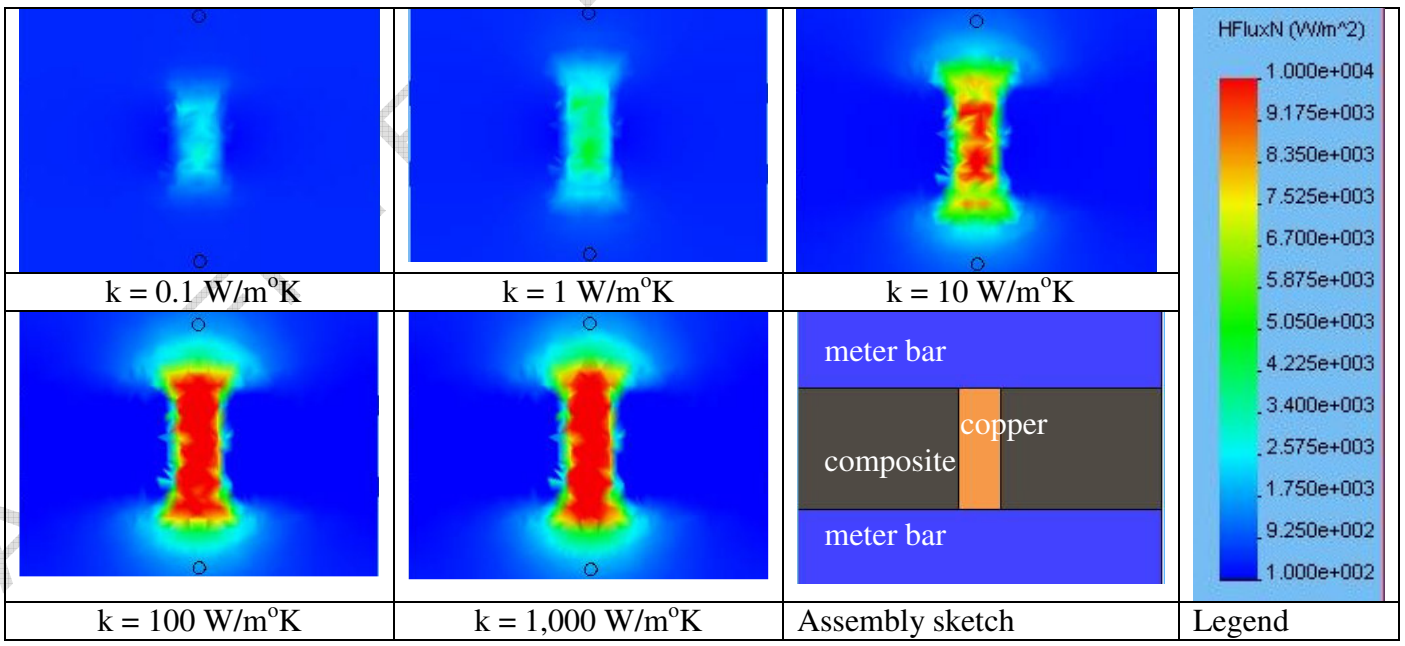

Figure 5: ***FEM-Results of heat flux depending on meter bar material's thermal conductivity***

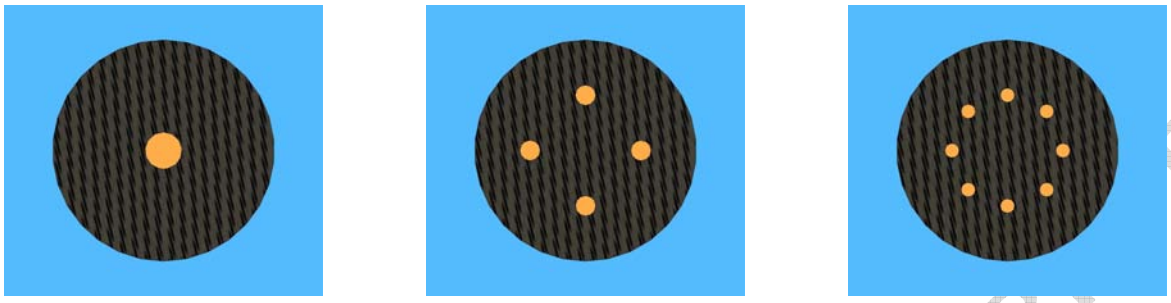

Figure 6: ***Composite sample with one, four, and eight copper fibers (v_{Cu} = 4.3 %)***

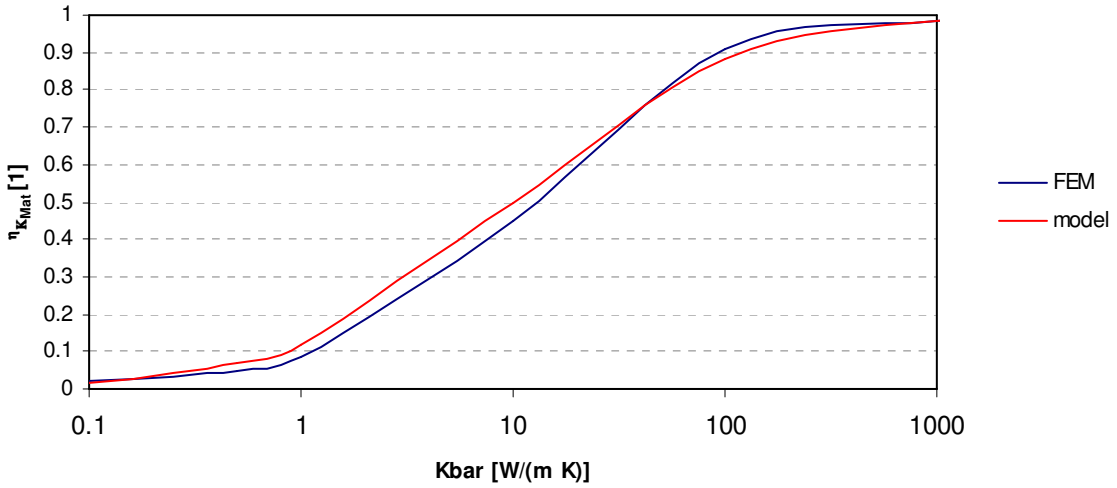

Figure 7: ***Dependency of η_{KMat} on meter bar material***

Table 3: ***Correlation between fiber distribution and thermal conductivity***

Number of Cu-fibers	Measured thermal conductivity [W/(m K)]
1	3.7
4	5.9
8	6.7

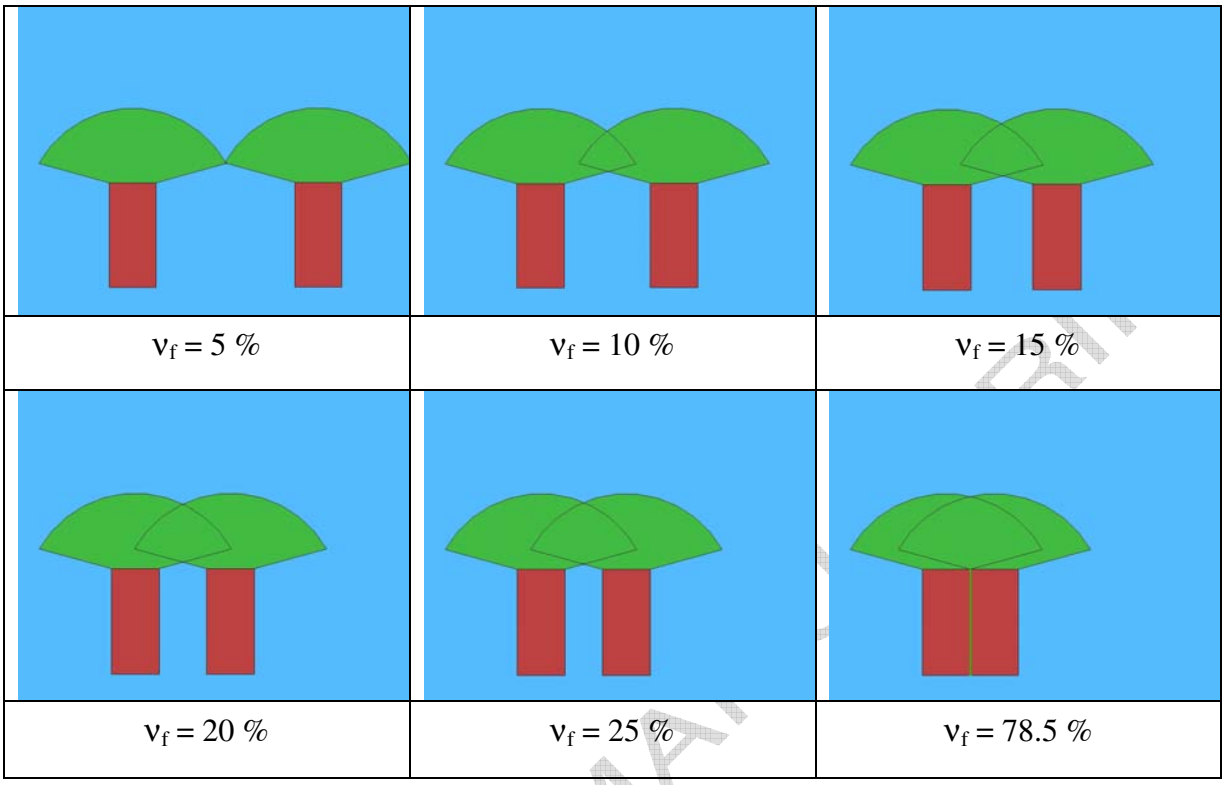

Figure 8: ***Overlapping of mushroom shaped heat flux area (K_{Mat} = 10 W/(m K))with varying z-fiber volume fraction***

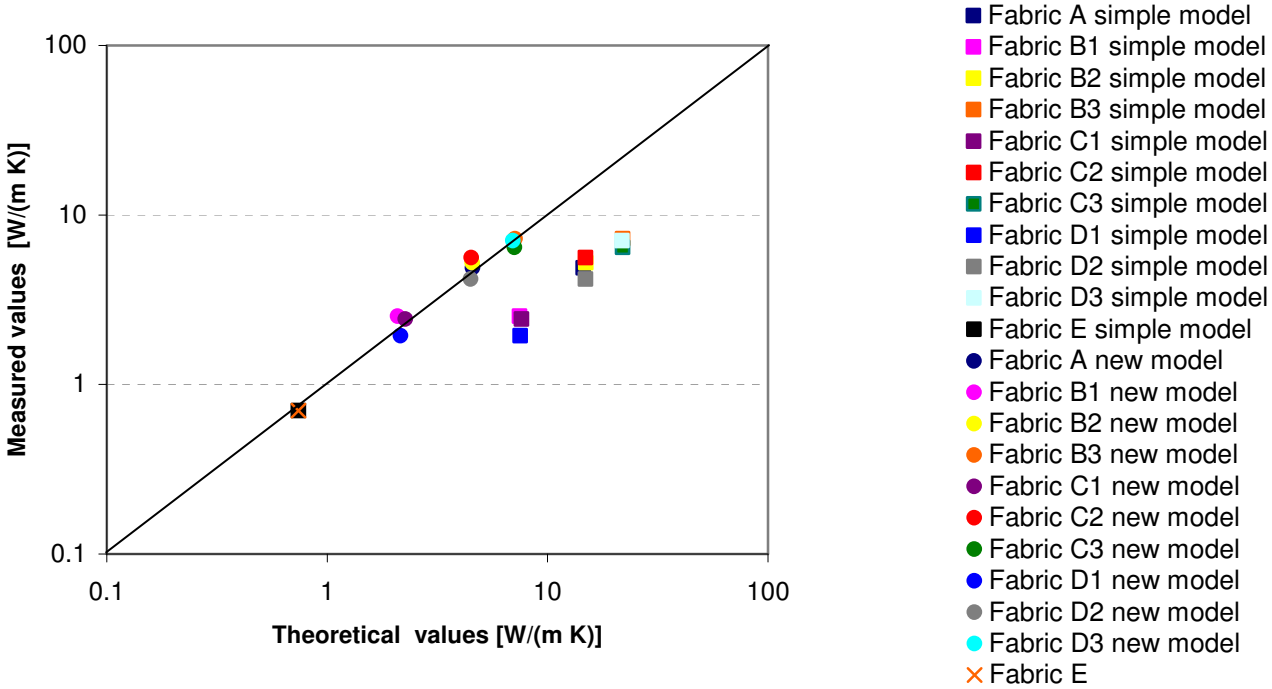

Figure 9: ***Comparison of simple rule of mixture values, new model and measured values***

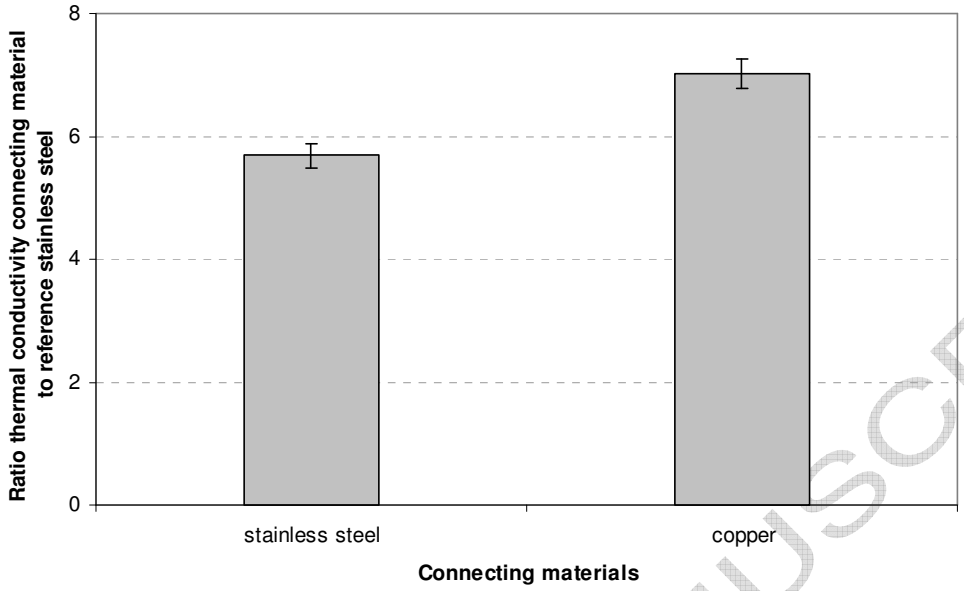

Figure 10: ***Influence of adjoining material on measured thermal conductivity***

Table 1: ***Thermal conductivity properties of sample constituents used [19, 21, 30]***

	base material	axial thermal conductivity K_a [W/(m K)]	radial thermal conductivity K_r [W/(m K)]
Cu-fiber	Copper	390	390
E-glass-fiber	glass	1.04	1.04
CN80-fiber	pitch	320	11
YS80-fiber	pitch	320	11
T300-fiber	PAN	100	11
T700-fiber	PAN	100	11
SC-15	epoxy	0.19	0.19

Table 2: ***Properties of 3WEAVE^{TM}-based composite samples***

	warp-fiber	fill-fiber	z-fiber	ν_F [%]	ν_{Fz} [%]	K [W/(m K)]
Matrix	-	-	-	0	0	0.19
Fabric A	T700	CN80	Cu	50	4,3	14.53
Fabric B1	T700	CN80	YS80	44	1.8	7.47
Fabric B2	T700	CN80	YS80	51	3,7	14.93
Fabric B3	T700	CN80	YS80	53	5.5	21.93
Fabric C1	T700	T300	YS80	56	1.8	7.63
Fabric C2	T700	T300	YS80	48	3.7	14.89
Fabric C3	T700	T300	YS80	50	5.5	21.90
Fabric D1	T700	E-glass	YS80	49	1.8	7.52
Fabric D2	T700	E-glass	YS80	45	3.7	14.85
Fabric D3	T700	E-glass	YS80	34	5.5	21.75
Fabric E	T300	T300	-	50	0	0.74

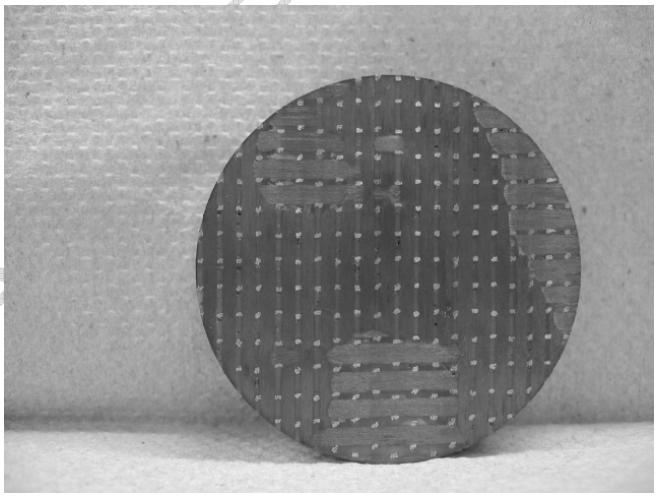

Figure 2: ***Exemplary sample for thermal conductivity measurements***